Chin. J. Mech. Eng. (2017) 30:301–309
DOI 10.1007/s10033-017-0071-y

ORIGINAL ARTICLE

Improved Soft Abrasive Flow Finishing Method Based on Turbulent Kinetic Energy Enhancing

Jun LI[1,2] · Shiming JI[1] · Dapeng TAN[1]

Received: 16 November 2016 / Revised: 28 December 2016 / Accepted: 3 January 2017 / Published online: 17 March 2017

Abstract Soft abrasive flow(SAF) finishing can process the irregular geometric surfaces, but with the matter of low processing efficiency. To address the issue, an improved SAF finishing method based on turbulent kinetic energy enhancing is proposed. A constrained flow passage with serration cross-section is constructed to increase the turbulence intensity. Taking the constrained flow passage as the objective, a two-phase fluid dynamic model is set up by using particle trajectory model and standard k-ε turbulence model, and the flow field characteristics of the flow passage are acquired. The numerical results show that the serration flow passage can enhance the turbulence intensity, uniform the particles distribution, and increase the particle concentration near the bottom wall. The observation results by particle image velocimetry(PIV) show that the internal vortex structures are formed in flow passage, and the abrasive flow takes on turbulence concentrating phenomenon in near-wall region. The finishing experiments prove that the proposed method can obtain better surface uniformity, and the processing efficiency can be improved more 35%. This research provides an abrasive flow modeling method to reveal the particle motion regulars, and can offer references to the technical optimization of fluid-based precision processing.

Keywords Soft abrasive flow · Serration flow passage · Kinetic energy enhancing · Particle image velocimetry

1 Introduction

With the rapid development of modern industry, new products require high standard moulds or workpieces with precise geometric size and uniform surface quality [1, 2]. With respect to the finishing for the surfaces of grooves, holes, prisms, pyramids, narrow channels and other irregular shapes, which are the so-called structural surfaces and involved a large number in mould manufacturing, the conventional finishing methods with rotating tools are hard to match the technical requirements of practical industry production [3, 4].

It is well known that the loose abrasive particles with multiple cutting edges can resolve the matter for the surfaces with irregular geometric shapes or complex structures. Accordingly, a no-tool fluid-based finishing method, i.e. the soft abrasive flow(SAF) finishing, is put forward [5, 6]. In the process of SAF finishing, abrasive particles in the fluid media are used as cutting tools acting on machining surfaces repeatedly, and the fluid media requires to be with intensive turbulent state. Apparently, SAF is a type of liquid-solid two-phase abrasive flow with a low effective viscosity, which has a better flow behavior with strong turbulence. The turbulence can be conducive to realize micro cutting with micro force to the structural surface of a mould for precision machining [7–9]. In view of the merits of the SAF finishing, it had been applied in

Supported by National Natural Science Foundation of China (Grant Nos. 51375446, 51575494), and Zhejiang Provincial Natural Science Foundation of China (Grant Nos. LR16E050001, LZ14E050001).

✉ Dapeng TAN
tandapeng@zjut.edu.cn

[1] Key Laboratory of E&M, Zhejiang University of Technology of Ministry of Education and Zhejiang Province, Hangzhou 310014, China

[2] School of Information Science and Engineering, Hangzhou Normal University, Hangzhou 311121, China

some engineering areas, such as mould manufacturing and automobile accessories [10–12].

In 2010, JI et al. developed a SAF dynamic model based on discrete phase method, and found that the abrasive flow processing was of variable processing efficiency caused by the influence of near-wall particle velocity [5]. In 2012, TAN et al. introduced the level set method(LSM) into fluid-based processing area, and proposed a modeling method for two-phase abrasive flow by LSM topological structure transformation. The method could analyze the motion regulars of the abrasive particles in turbulent state, and trace the interface variation regulars of two-phase abrasive flow [6]. LI et al. presented a fluid mechanic model for SAF near-wall region. The model adopted Nikuradse's experimental methods to acquire the variation regulars of SAF turbulent parameters and flow passage pressure profiles with different inlet velocities [13]. In 2013, ZENG, et al. put forward a material removal model by the modified Preston equation. According to a series of simulation and practical experiments, the size of abrasive, hardness of abrasive, and hardness of surface were derived as important factors for the material removal. The processing results showed that the modified Preston equation was propitious to avoid errors for calculation [14]. In 2014, JI, et al. set up an ultrasound-based SAF processing apparatus to improve the processing efficiency and surface quality. The processing experiments showed that there are large numbers of bubbles that were growing and hitting on the wall continuously, and the SAF coupled with ultrasound wave could reduce the processing time effectively [15]. In 2016, TAN, et al. proposed a double-inlet SAF finishing method based on the fluid collision theory. The processing experiments showed that the double-inlet SAF finishing method could improve the finishing uniformity and efficiency [16]. ZENG et al. adopted the soft ball model to analyze the normal and shear contact forces between two particles. By introducing damping coefficient, formulas on displacement and velocity were given for theory analysis of creep deformation. Then, the force chains were established by simulation, which proves that softness consolidation abrasives possess more cutting force than free abrasives [17]. KAVITHAA et al. proposed a model to describe the nanometric surface finishing of typical prosthetic implants and an extrusion die used in bio-medical and pharmaceutical industries, respectively. The finishing and deburring for a propeller and a shuttle valve used in aerospace applications are performed [18].

Although the SAF finishing method is of many benefits, the soft abrasive flow mechanism with dilute particles in complicated constrained channels is with high nonlinearity, and still remains unclear. Moreover, owing to the low particle fraction of SAF, the processing efficiency require to be improved.

From the above references, it can be inferred that particle motion mechanism is a difficult point of two-phase abrasive flow, and with inherent relations to the internal energy distribution, i.e. the turbulent kinetic energy. Therefore, this paper introduces the particle trajectory model into the SAF dynamic modeling area, in which the particle concentration is 10%. Based on the above hypothesis, a constrained flow passage with serration cross-section is constructed to increase the turbulence intensity of abrasive flow, and the processing efficiency of SAF finishing will be improved.

The main scientific contribution of the paper is providing an abrasive flow dynamical modeling method for particle motion regulars, and promoting an improved SAF finishing method to increase the processing efficiency. The research work not only can provide direct suggestions for the researchers of the fluid-solid contacting matters of constrained or non-constrained fluidic processing methods, but also can offer universal references to the engineering areas of large-scale hydraulic machinery design, chemical reactor internal state monitoring and fluid-solid coupling resistance optimization.

2 SAF Fluid Dynamic Model

Particles motion is an important issue to research the processing mechanism of SAF, and reveal the corresponding dynamical regulars. It focuses on the momentum transfers between particles and the processing media, i.e. the fluid phase. The liquid phase is usually considered to be continuous as the particle phase, and with two dynamic modeling methods. The first one is behaved under the Euler conference frame, and the particles are considered as quasi fluid that can be regarded as the discrete phase. In this assumption, the two-phase flow simulation for liquid and particle phase is also called two-fluid model, but is not applicable to the dilute particle-liquid flow. The other is particle trajectory model under the Lagrange conference frame. In combination with the continuous liquid phase model, it constitutes the Euler-Lagrange model to solve the Navier-Stokes(N-S) equation [19–22]. Accordingly, if the continuous liquid phase flow field is obtained, the force of particles is calculated together with flow field to obtain the particles velocity, in which the trajectory tracking for each particle is regarded as the discrete phase. This approach assumes that the concentration of the discrete phase is generally less than 10%–15%, so the interaction between particles and the influence of the particle volume fraction on the continuous phase can be ignored.

2.1 Liquid Phase Governing Equations

As mentioned above, SAF is a kind of two-phase incompressible fluid with lower particle phase concentration, where continuous equation of the fluid phase is [5, 6]

$$\frac{\partial(\rho_k\alpha_k)}{\partial t}+\nabla\bullet(\rho_k\alpha_k u_k)=0. \tag{1}$$

The momentum conservation equation of the continuous phase is

$$\begin{aligned}&\frac{\partial}{\partial t}(\rho_k\alpha_k u_k)+\mu\bullet\nabla(\rho_k\alpha_k u_k)\\&\quad=-\alpha\nabla p+\rho_k\alpha_k g+\nabla\left[\mu_{eff}\nabla u_k\right]+F_k+S_k.\end{aligned} \tag{2}$$

In Eqs. (1) and (2), ρ_k is the density of fluid phase, α_k is the liquid volume fraction, t is the time variable, u_k is the velocity of liquid phase, μ is the kinetic viscosity, p is the pressure of the fluid phase, F_k is the force between the phases, g is the acceleration of gravity, and S_k is the source term written in the general form.

2.2 Particle Phase Motion Equations

By calculating the integral of the force balance equation of particles under the Lagrange coordinates, the trajectories of discrete phase particles can be obtained. In this paper, since the particles concentration is rather low, the basset force, virtual mass force, magnus force, saffman force and buoyancy force [13–15] in particle motion equation are ignored, and only the gravity and drag force are considered. The particle motion equation is as follows:

$$\frac{\mathrm{d}u_\mathrm{p}}{\mathrm{d}t}=F_D(u-u_p)+\frac{g(\rho\rho_p-\rho)}{\rho_p}, \tag{3}$$

the first term of the right hand of Eq. (3) is the drag force on per unit mass of the particle, and the F_D can be written as

$$F_D=\frac{18\mu}{\rho_p d_p^2}\frac{C_D\mathrm{Re}}{24}, \tag{4}$$

where u is the fluid phase velocity, u_p is the particle velocity, ρ is the fluid density, ρ_p is the particle density, g is the additional acceleration, d_p is the particle diameter, and R_e is the particle Reynolds number:

$$R_e=\frac{\rho d_p|u_p-u|}{\mu}, \tag{5}$$

the drag coefficient C_D is given as [13]

$$C_D=\left(0.63+\frac{4.8}{\mathrm{Re}_p^{0.5}}\right)^2. \tag{6}$$

2.3 Turbulence Model

Turbulence is the key feature of SAF, and is the pre-condition to guarantee the processing effects of SAF finishing method. Considering the matter, the fluid mechanic model requires to involve the turbulence model, in which the equations of the turbulent kinetic energy and the dissipation rate are as follows:

$$\frac{\partial(\rho k)}{\partial t}+\frac{\partial(\rho k u_i)}{\partial x_i}=\frac{\partial}{\partial x_j}\left[\left(\mu+\frac{\mu_t}{\sigma_k}\right)\frac{\partial k}{\partial x_j}\right]+G_k-\rho\varepsilon, \tag{7}$$

$$\begin{aligned}\frac{\partial(\rho\varepsilon)}{\partial t}+\frac{\partial(\rho\varepsilon u_i)}{\partial x_i}&=\frac{\partial}{\partial x_j}\left[\left(\mu+\frac{\mu_t}{\sigma_\varepsilon}\right)\frac{\partial\varepsilon}{\partial x_j}\right]hfill\\&\quad+\frac{C_{1\varepsilon}\varepsilon}{k}G_k-C_{2\varepsilon}\rho\frac{\varepsilon^2}{k},\end{aligned} \tag{8}$$

$$G_k=\mu_t\left(\frac{\partial u_i}{\partial x_j}+\frac{\partial u_j}{\partial x_i}\right)\frac{\partial u_i}{\partial x_j}, \tag{9}$$

$$\mu_t=\rho C_\mu\frac{k^2}{\varepsilon}. \tag{10}$$

In Eqs. (7)–(10), k is the turbulent kinetic energy, ε is the dissipation rate, μ_t is the turbulent viscosity, G_k is the turbulent kinetic energy caused by the average velocity gradient, $C_{1\varepsilon}$, $C_{2\varepsilon}$, C_u are the experience constant with the value of 1.44, 1.92, 0.09 respectively, σ_ε, σ_k are the Prandtl numbers corresponding to the turbulent kinetic energy and the turbulent dissipation rate with the value of 1.0 and 1.3, respectively.

3 Objective Physical Model and Boundary Conditions

3.1 Physical Model

As shown in Fig. 1, the processing apparatus of SAF finishing is composed of four kernel parts: fixture, constrained module, base entity and workpiece. As indicated above, the constrained module is with serration cross-section, and constructs the constrained flow passage with workpiece.

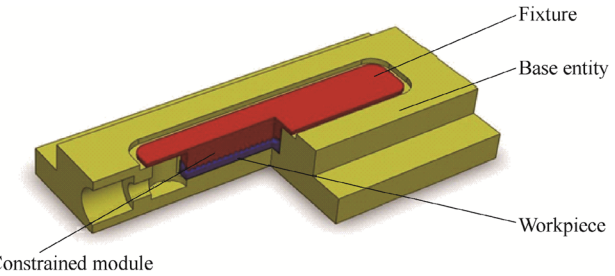

Fig. 1 Structural diagram of the SAF processing apparatus

The geometric sizes of the flow passage are as follows: length (100 mm), width (12 mm), and height (2 mm). In the flow passage, SAF is extruded by a pump and form turbulence state, and the micro-force and micro cutting effects are performed on the surface of workpiece.

For the above objective, the grid meshing with unstructured hexahedral units is implemented by ANASYS-FLUENT®, as shown in Fig. 2. The calculation region is the flow passage, and the length is 100 mm. The total grid number is about 790 920. In order to guarantee the modeling repeatability, and the grid independent verification is performed.

3.2 Boundary Conditions

Considering the grid model of constrained flow passage, the boundary conditions can be defined as follows. The inlet boundary is set as velocity entrance while the outlet is outflow. The particles are put at the entrance of the flow channel with the velocity vector direction perpendicular to the cross-section. Discrete particles random orbital model is used considering the interphase coupling effect between continuous liquid phase and discrete particles. The equations are solved by the phase coupled SIMPLE algorithm employing pressure and velocity coupling with the first-order upwind discrete format. The iteration time step is 0.000 1 s.

The liquid phase is selected as 46# engine oil with the initial velocity of 60 $m{\cdot}s^{-1}$, assuming the flow has been fully developed into turbulent flow. The turbulence intensity can be given as

$$I = 0.16(\mathrm{Re}_{DH})^{-1/8} = 5.2\%. \tag{11}$$

The solid phase is SiC particles of which the average diameter is 55 μm. The density and the dynamic viscosity are 3170 $kg{\cdot}m^{-3}$ and 2.064×10^{-6} $m^2{\cdot}s^{-1}$, respectively. The initial velocity is set to be 60 $m{\cdot}s^{-1}$and the mass flow rate is 1.03 $kg{\cdot}s^{-1}$ with the volume fraction of 10%. The wall function method and no-slip boundary conditions are used for the liquid phase. For the particle phase, the non-equilibrium wall function approximation is used in the area near the wall.

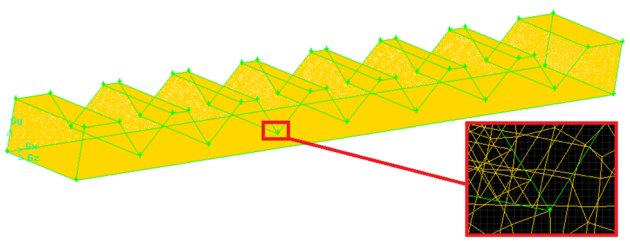

Fig. 2 Grid meshing of the constrained flow passage

4 Numerical Simulation and Results Discussion

Relative research works [13–17] prove that the processing effects for a structured surface in constrained flow passage is closely related with the particle velocity, pressure and other flow field parameters. Therefore, the velocity profiles, turbulence properties and the particle dynamic characteristics are mainly analyzed in the serration shape flow passage.

According to the SAF dynamic model in Section 2, the transverse velocity profile of constrained flow passage is obtained, as shown in Fig. 3. Owing to the resistance and disturbance effects of constrained module, the high-velocity region is shifted to the bottom of flow passage, i.e. the near-workpiece region with higher velocity amplitude, which is helpful to improve the processing efficiency.

Figure 4 shows the velocity distribution along the flow passage direction near the bottom wall which is the machining surface of the workpiece. The velocity from the position of 0.015 m to 0.095 m is displayed almost in sine curve shape, with the minimum value of 60 $m{\cdot}s^{-1}$ and the maximum value of 110 $m{\cdot}s^{-1}$. It indicates that the velocity near the wall in the flow channel changes continuously. This alternating velocity field can be advantageous for micro cutting effect of the particles with micro force on the workpiece surface with much more machining precision.

The turbulent kinetic energy reflects the length and time scale of turbulence pulse in the flow channel (shown in Fig. 5), which is one of the important factors to the finishing effects. If the turbulent kinetic energy of abrasive flow becomes larger, the pulse intensity will be higher. Because the simulated iteration of the flow field in the constrained passage enters stable state at less than 0.03 s, the 0.05 s is selected as the observation time point of simulation results.

Figure 6 shows the velocity vector distribution of the grinding particles group in the constrained flow passage for the iteration time of 0.05 s. It can be seen that the distribution of the grinding particles is uniform along the x-direction and the particles are much more concentrated near

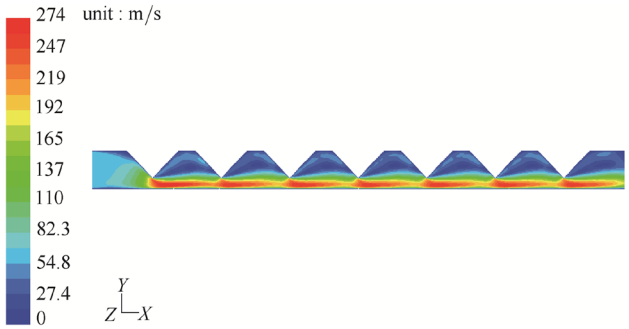

Fig. 3 Transverse velocity profile of flow passage

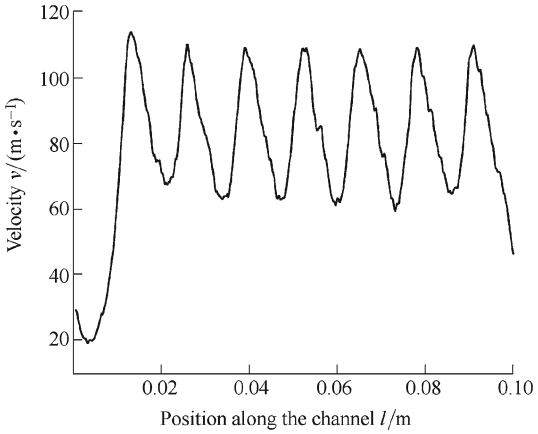

Fig. 4 Velocity distribution near the bottom wall

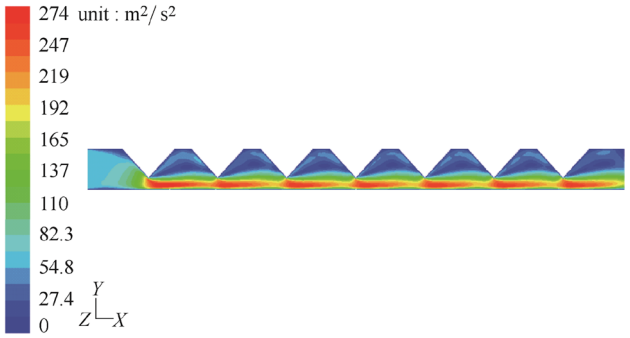

Fig. 5 Contours of turbulent kinetic energy

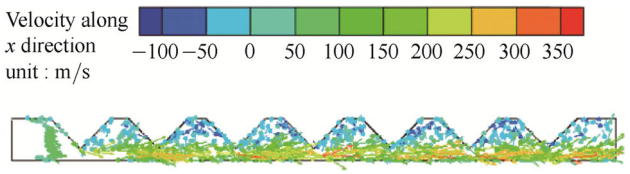

Fig. 6 Velocity vector distribution of particles

the bottom wall area with larger relative velocity. The vortex exists between two grooves, which indicates that the grinding particles have reached a disordered turbulent state.

To acquire the global profile of particle motion, the 3D vector distribution of the particles is shown in Fig. 7. In the figure, there is a clear and frequent collision trend for the grinding particles to the wall, with a disorder distribution. Apparently, the disorder motion can change the directions of processing tracks, and the processing uniformity will be improved.

Processing effects of SAF finishing are the final targets of numerical simulation, so the simulated abrasion for the workpiece surface is shown in Fig. 8. It indicates that the surface abrasion gradually increases along the channel from the entrance, and eventually reaches a uniform wear at the outlet. If the constrained module moves along the

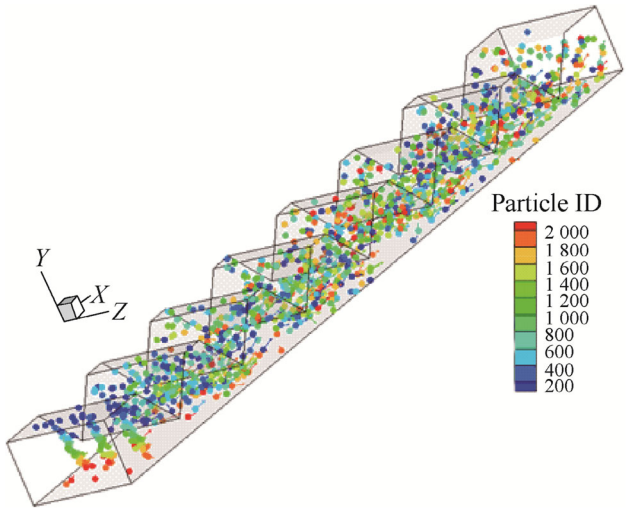

Fig. 7 3D vector distribution of particles

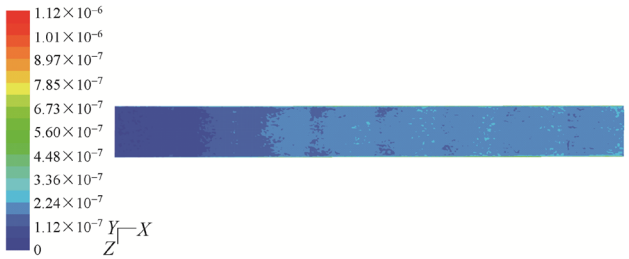

Fig. 8 Wear of workpiece machining surface'

passage direction, the uniform machining to the workpiece surface would be achieved.

5 Experimental Verifications

5.1 PIV Observation Experiments

As indicated above, particle motion is a key factor to the processing effects of SAF finishing. To verify the numerical results of particle motion, a PIV based observation experimental platform is established [23–25], as shown in Fig. 9.

The experimental platform is composed of four functional components: a high-frequency laser transmitter, a high-speed camera, a constrained flow passage and a PIV post-processing system. To observe the internal flow field of constrained flow passage, the constrained flow passage is constructed by transparent materials. The processing procedures of PIV observation for particle motion in flow passage are described as follows. Firstly, the two single particle images are divided into small areas. Then the cross-correlation analysis is applied to the two particle images on the area to get the velocity vectors, and finally

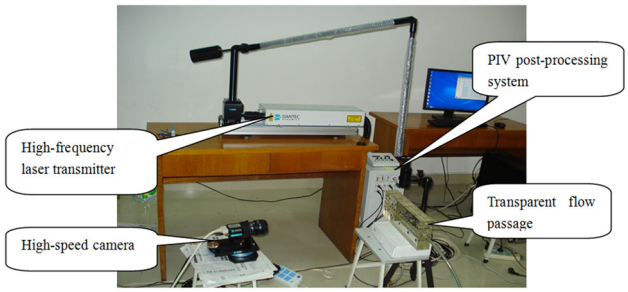

(a) PIV observation system

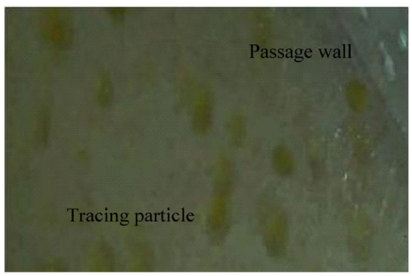

(b) Amplification photo of transparent flow passage

Fig. 9 SAF observation experimental platform

the velocity vectors of the total area are obtained. Figure 10 shows the distribution of the particles in the constrained flow passage.

Figure 10 shows that the distribution of the particles is approximately uniform along the axial direction. By processing the local area of the images within the red rectangle window as shown in Fig. 10, the local velocity vector diagram of the grinding particles is obtained, as shown in Fig. 11. It shows that some internal vortex structures are formed in the flow filed. The vortex movement makes the particles accelerate and decelerate constantly and disturbs the particles flow state near the wall boundary layer. Therefore, the abrasive flow takes on turbulence concentrating phenomenon in the near-wall region. The consequent turbulence of the SAF in constrained flow channel will help the particles cut the workpiece surface with disorderly micro forces. The above results accord with the numerical simulation results in Fig. 6 and Fig. 7.

5.2 Processing Experiments

In order to check the effectiveness of the proposed SAF finishing method, a processing experimental platform is developed, as shown in Fig. 12. The experimental platform

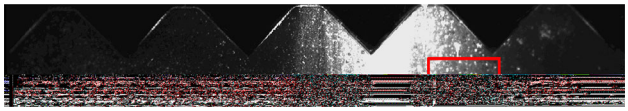

Fig. 10 Distribution of particles in the flow channel

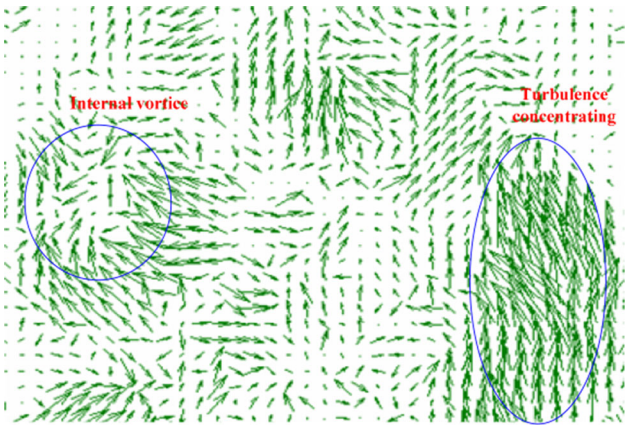

Fig. 11 Local velocity vector of particles

Fig. 12 SAF processing experimental platform

contains a fixture apparatus, a constrained flow passage, a SAF agitator and a diaphragm pump. The dimension, structure and processing condition of the constrained flow channel processed in the experiment are the same as those in the numerical simulation.

The workpiece for the processing experiment is made of 45# steel, and with the geometric size of 100 mm × 12 mm × 5 mm. The constrained module is with serration shape structure, and it constructs the constrained flow passage with the workpiece and the steel base entity, as shown in Fig. 13.

To guarantee the mass transformation performance of constrained flow passage, the average gap of the passage is 2 mm. The initial surface roughness value *Ra* of the testing workpiece is 3 μm. The processing media with the grinding particles is the mixture of #46 hydraulic oil and the green silicon carbide particles with the average diameter of 55 μm. The total mass of the solid particles is 2.5 kg. The mixture is stirred by the agitator during the entire experiment before entering the finishing section to ensure the liquid phase blend well with the particles. The initial velocity of the particles flow is 60 $m \cdot s^{-1}$, and the particle volume fraction is about 10%.

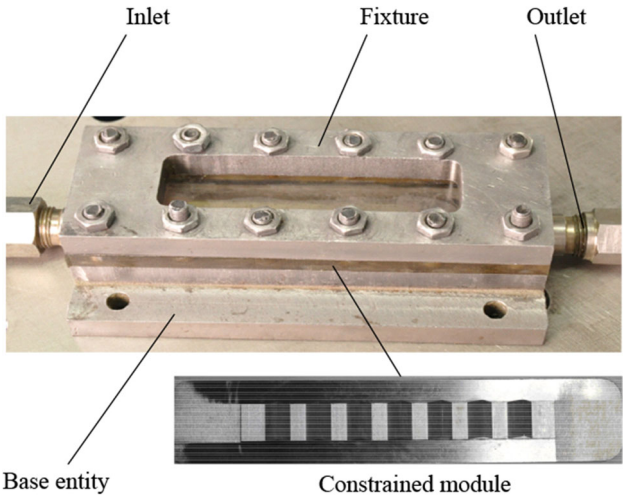

Fig. 13 SAF processing apparatus with serration shape constrained module

The surface roughness values for the testing workpiece are measured every three hours during the experiment. The measuring locations with the total number of 13 are regularly distributed on the surface of the workpiece along both the transverse and longitudinal direction, corresponding to the embossments and grooves of the serration shape structure. After 21 h processing, the surface quality variation is shown in Fig. 14. From the figure, we can find that the proposed method can obtain better surface roughness and uniformity.

To acquire the detail data and global profile of surface roughness, the 3D distribution of the surface roughness values for the testing workpiece is obtained, as shown in Fig. 15. It can be seen that the average peak roughness values on the surface of the testing workpiece drop a lot obviously and the surface becomes smooth after it has been processed for 21 h, indicating the good processing effects.

Subsequently, for verifying the advantages of processing efficiency of the proposed SAF finishing method, two groups of comparative experiments with traditional SAF finishing method have been performed, and the results are shown in Table 1 and Table 2. It can be seen that less processing time is consumed for the same surface roughness by using the proposed SAF finishing method. Apparently, owing to the turbulent energy enhancing, the proposed method can improve the processing efficiency more 35%.

Moreover, to check the surface quality of the proposed method, the comparative experiments for flatness have been implemented. Similarly, the proposed method can perform better processing efficiency, also accompanied with on manifest performance advantages. Because SAF processing is for the finishing stage of workpiece, it is with limited ability to improve the geometric tolerance.

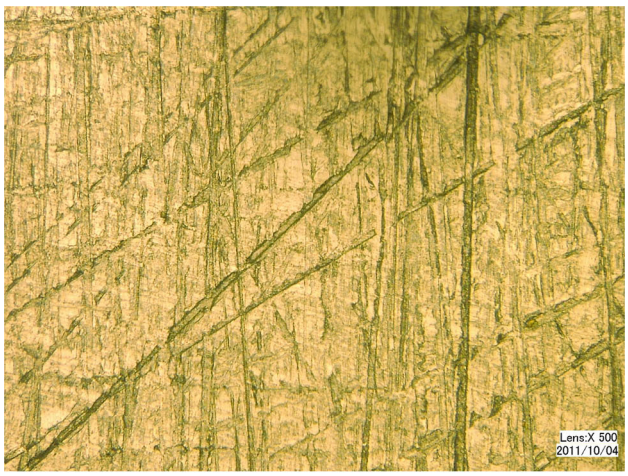

(a) Before processing

(b) After processing

Fig. 14 Comparison of surface quality for the testing workpiece

6 Conclusions

(1) The concentration of the grinding particles is rather low at the entrance of the whole flow passage. The distribution of the particles becomes uniform with the disorderly particle velocity vectors at the middle segment and the outlet. The two-phase flow in the flow passage has reached the turbulent state, which is beneficial to the processing effects.

(2) Near the bottom surface of the passage, the turbulent kinetic energy is much more uniform and larger, which indicates that the turbulent pulse strength and velocity are larger as well. Thus the cutting intensity of the grinding particles to the workpiece surface is stronger and much more frequent and disordered, resulting in the improvement of the machining efficiency.

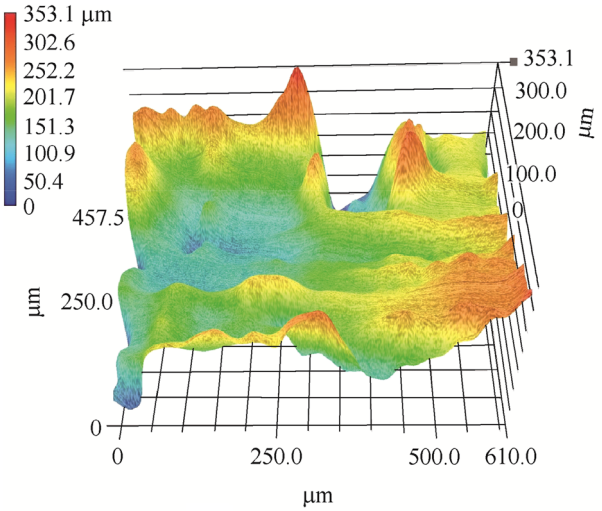

(a) Before processing

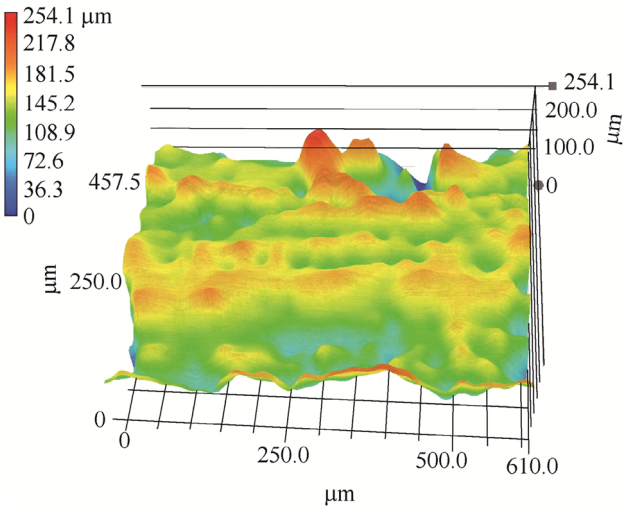

(b) After processing

Fig. 15 Comparison of 3D morphology for testing workpiece

Table 1 Processing time of traditional method at different surface roughness (h)

Exp.	Surface roughness *Ra*/μm			
	1.0	0.5	0.3	0.15
Group-1	5.5	20.5	25.5	35.5
Group-2	7.0	21.5	27.5	36

(3) By using the PIV techniques, the observation results of the distribution and the velocity vectors of the grinding particles in the constrained flow passage have been obtained, verifying the simulated results.

(4) A processing experimental platform is established, and the processing experiments have been finished.

Table 2 Processing time of proposed method at different surface roughness (h)

Exp.	Surface roughness *Ra*/μm			
	1.0	0.5	0.3	0.15
Group-1	3.5	12.5	17.5	22
Group-2	4.5	13	18	21.5

The results show that the proposed SAF finishing method can obtain better surface quality and processing efficiency.

References

1. HUANG Y H, GU L Z. Digitalized accurate modeling of SPCB with multi-spiral surface based on CPC algorithm[J]. *Chinese Journal of Mechanical Engineering*, 2015, 28(5): 1039–1047.
2. LI Y B, TAN D P, WEN D H, et al. Parameters optimization of a novel 5-DOF gasbag polishing machine tool[J]. *Chinese Journal of Mechanical Engineering*, 2013, 26(4): 680–688.
3. SANKAR M R, JAIN V K, RAMKUMAR J. Rheological characterization of styrene-butadiene based medium and its finishing performance using rotational abrasive flow finishing process[J]. *International Journal of Machine Tools and Manufacture*, 2011, 51(12): 947–957.
4. ZENG X, JI S M, JIN M S, et al. Investigation on machining characteristic of pneumatic wheel based on softness consolidation abrasives[J]. *International Journal of Precision Engineering and Manufacturing*, 2014, 15(10): 2031–2039.
5. JI S M, XIAO F Q, TAN D P. Analytical method for softness abrasive flow field based on discrete phase model[J]. *Science China - Technological Sciences*, 2010, 53(10): 2867–2877.
6. JI S M, WENG X X, TAN D P. Analytical method of softness abrasive two-phase flow field based on 2D model of LSM[J]. *Acta Physica Sinica*, 2012, 61(1): 10205.
7. TAN D P, LI P Y, PAN X H. Application of improved HMM algorithm in slag detection system[J]. *Journal of Iron and Steel Research, International*, 2009, 16(1): 1–6.
8. TAN D P, LI P Y, JI Y X, et al. SA-ANN-based slag carry-over detection method and the embedded WME platform[J]. *IEEE Transactions on Industrial Electronics*, 2013, 60(10): 4702–4713.
9. TAN D P, JI S M, LI P Y, et al. Development of vibration style ladle slag detection method and the key technologies[J]. *Science China - Technological Sciences*, 2010, 53(9): 2378–2387.
10. JI S M, XIAO F Q, TAN D P. A new ultraprecision machining method with softness abrasive flow based on discrete phase model[J]. *Advanced Materials Research*, 2010, 97–101: 3055–3059.
11. YUAN Q L, JI S M, TAN D P, et al. Analytical method for softness abrasive flow field based on low Reynolds *k*-epsilon model[J]. *Advanced Materials Research*, 2011, 188: 230–235.
12. JI S M, ZHONG J Q, TAN D P, et al. Research of distribution and dynamic characteristic of particle group in the structural flow passage[J]. *Key Engineering Materials*, 2012, 499: 271–276.
13. LI C, JI S M, TAN D P. Softness abrasive flow method oriented to tiny scale mold structural surface[J]. *International Journal of Advanced Manufacturing Technology*, 2012, 61: 975–987.
14. ZENG X, JI S M, TAN D P, et al. Zhang. Softness consolidation abrasives material removal characteristic oriented to laser

hardening surface[J]. *International Journal of Advanced Manufacturing Technology*, 2013, 69(9–12): 2323–2332.
15. JI S M, QIU Y, CAI Y J, et al. Research on mechanism of ultrasound enhancing and the experiment based on softness abrasive flow[J]. *Chinese Journal of Mechanical Engineering*, 2014, 50(4): 84–93.
16. TAN D P, JI S M, FU Y Z. An improved soft abrasive flow finishing method based on fluid collision theory[J]. *International Journal of Advanced Manufacturing Technology*, 2016, 85(5–8): 1261–1274.
17. ZENG X, JI S M, JIN M S, et al. Research on dynamic characteristic of softness consolidation abrasives in machining process[J]. *International Journal of Advanced Manufacturing Technology*, 2016, 82(5–8): 1115–1125.
18. KAVITHAA T S, BALASHANMUGAM N. Nanometric surface finishing of typical industrial components by abrasive flow finishing[J]. *International Journal of Advanced Manufacturing Technology*, 2016, 85(9–12): 2189–2196.
19. CHEN J L, XU F, TAN D P, et al. A control method for agricultural greenhouse heating based on computational fluid dynamics and energy prediction model[J]. *Applied Energy*, 2015, 141: 106–118.
20. TAN D P, JI S M, JIN M S. Intelligent computer-aided instruction modeling and a method to optimize study strategies for parallel robot instruction[J]. *IEEE Transactions on Education*, 2013, 56(3): 268–273.
21. TAN D P, ZHANG L B. A WP-based nonlinear vibration sensing method for invisible liquid steel slag detection[J]. *Sensors and Actuators B - Chemical*, 2014, 202: 1257–1269.
22. TAN D P, YANG T, ZHAO J, et al. Free sink vortex Ekman suction-extraction evolution mechanism [J]. *Acta Physica Sinica*, 2016, 65(5): 054701.
23. TAN D P, LI P Y, PAN X H. Intelligent industry monitoring network architecture UPnP based[J]. *Chinese Journal of Electronics*, 2008, 17(4): 607–610.
24. LI C, JI S M, TAN D P. Multiple-loop digital control method for 400 Hz inverter system based on phase feedback[J]. *IEEE Transactions on Power Electronics*, 2013, 28(1): 408–417.
25. HU C L, WANG G Y, HUANG B A. Experimental investigation on cavitating flow shedding over an axisymmetric blunt body[J]. *Chinese Journal of Mechanical Engineering*, 2015, 28(2): 387–393.

Jun LI born in 1982, is currently a PhD candidate at *Zhejiang University of Technology, China.* He received his master degree from *Beijing University of Posts and Telecommunications, China*, in 2008. His research interests include ultra precision machining and industrial testing technology. E-mail: 20050040@hznu.edu.cn.

Shiming JI born in 1957, is currently a professor at *Zhejiang University of Technology, China*. He received his PhD degree from *Zhejiang University, China*, in 2000. His research interests include ultra precision machining, image processing and parallel robot. E-mail: jishiming@zjut.edu.cn.

Dapeng TAN born in 1980, is currently a professor at *Zhejiang University of Technology, China.* He received his PhD degree from *Zhejiang University, China*, in 2008. His research interests include mechatronic engineering, ultra precision machining and embedded system technology.